

## Chapter 9

# The Young Stars

The entity that emerges from a core is a young star that only vaguely resembles the final version. It is spinning, spotted and oversized. The core and envelope have been shed but a massive disk now dominates the environment. In this chapter, we describe and explore the reasons for the violent behaviour and how it is eventually harnessed.

The vast majority of young stars are T Tauri stars. This is simply because they spend most time in this slowly evolving state. It can be argued that the destiny of T Tauri stars has been pre-determined in the previous collapse and main accretion stages. Therefore, this growing phase represents nothing more than a necessary stage to endure in the progress towards adulthood. However, they prove to be of immense observational significance. As objects revealed in the optical for the first time, they have provided most of our knowledge of Young Stellar Objects (YSOs). Due to their large numbers, however, they also provide us with statistical samples and spatial distributions. Finally, we find that both accretion and outflow have not been entirely eradicated but are still ongoing in a moderate form. This activity thus presents itself in manifestations explorable with our optical telescopes.

As planet-forming environments, the classical T Tauri stars have now taken on extra significance. We can explore how a spinning disk might evolve out of an envelope into a stellar system in which a star is surrounded by planets. The disk geometry and the balance of forces permit a more quantitative approach here than for any other stage of star formation. Our concepts concerning the nature and evolution of proto-planetary disks can now be tested. This has led us to re-think our ideas because observations have revealed unexpected disk properties.

## 9.1 T Tauri Stars

### 9.1.1 Classical T Tauri stars

In 1945, Alfred Joy classified a group of 11 stars as ‘T Tauri variables’, named after the prototype discovered in the constellation of Taurus. They displayed erratic optical variability, strong chromospheric lines and could be identified through their strong  $H\alpha$  emission lines. They were found to congregate at the periphery of dark clouds. The nearest were located in the Taurus molecular cloud and the  $\rho$  Ophiuchus cloud. Given our present knowledge, they clearly represent an early stage in the evolution of stars of low mass (less than  $3 M_{\odot}$ ) that are similar to the Sun.

Stars which resemble the original group are now referred to as Classical T Tauri stars (CTTSs). Their temperatures and masses are similar to the Sun but they are considerably brighter. They have been found to possess many extraordinary properties, in comparison to which the Sun is mild-mannered and mature. Their outstanding properties, discussed in detail below, include the following:

- They spin rapidly, with typical rotation periods of 1–8 days, compared to about a month for the Sun (25.6 days at the equator and about 36 days in the polar regions).
- Large areas of the surface are covered by hot starspots, typically 3–20% whereas the cool Sun spots usually cover a few tenths of a per cent of the solar surface.
- Variable emission occurs in the X-ray and radio bands (a thousand times stronger than solar-like activity).
- Strong stellar winds and collimated outflows are usually found ( $10^6$  times stronger than the solar wind of  $10^{-14} M_{\odot} \text{ yr}^{-1}$ ). The outflows are often associated with spectacular jets (see §9.8).
- Their external environments are complex. Classical T Tauri stars are surrounded by gas disks, revealed through strong excess emission in the infrared and sub-millimetre (see also Fig. 9.1).
- Most T Tauri stars are in binary star systems (see §12.2.1).

Since these stars are exposed at visible wavelengths, optical spectroscopy provides strong constraints on our interpretation. Ultraviolet observations with the International Ultraviolet Explorer (IUE) revealed high levels of line emission that are typical of the chromosphere and transition regions of the Sun, in addition to the hydrogen Balmer lines, calcium (H and K lines)

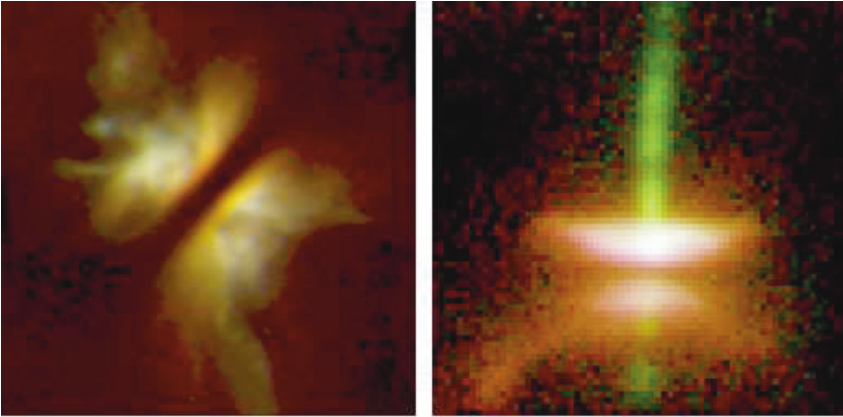


Fig. 9.1 These Hubble Space Telescope images show stars surrounded by dusty disks. You cannot see the star in either photograph, though their light illuminates the surrounding nebula. Left: Image of a star called IRAS 04302 2247. Right: in HH 30, jets emanate from the centre of a dark disk of dust which encircles the young star. The surfaces of the disk can be seen in reflected light. (Credit: NASA, HST, D. Padgett *et al.* 1999, AJ 117, 1490; C. Burrows *et al.* 1996, ApJ 473, 437.)

and various forbidden emission lines. Such lines have traditionally been used to find CTTs using objective prism techniques. Now, multi-object spectroscopy employing optical fibre technology allows us to survey wide regions quite efficiently.

We now recognise that the hydrogen lines are not actually produced as on the Sun but within an extended dense wind and accretion flow. A strong fast wind is deduced from the Doppler line shifts and widths of the  $H\alpha$  and forbidden lines (e.g. from once-ionised sulphur and neutral oxygen). These lines are often blue-shifted. The absence of red-shifted emission is interpreted as due to occultation of the far side by an opaque disk.

Excess ultraviolet and blue emission often disguise the spectral characteristics of Classical T Tauri stars. The cause is believed to be related to the manner in which material falls from the inner edge of the accretion disk onto the star. The effect is to ‘veil’ photospheric absorption lines. That is, the absorption lines are less deep than standard stars of the same spectral type. A significant observation is that the veiling is only present if the near-infrared excess is also present.

There are also several T Tauri stars in Taurus whose optical spectra are too heavily veiled to enable detection of the photospheric features needed for

spectral classification. These stars are typically referred to as ‘continuum’ stars.

Ultraviolet emission lines originating from hydrogen molecules have now been identified in a large sample of Classical T Tauri stars. These lines are probably the consequences of resonant fluorescence of molecular hydrogen following excitation from either atomic hydrogen Lyman  $\alpha$  photons or pumping from other atomic transitions. The origin of the emission could be either disk or nebular material surrounding the stars. Since  $\text{H}_2$  is the most abundant species in the disk, analysis of its physical conditions has important implications for a wide range of topics.

In summary, classical T Tauri stars are viewed as composite systems, comprising of an active stellar photosphere, an accretion zone, an extended circumstellar disk of cool material and atomic jets.

### 9.1.2 *Weak-line T Tauri stars*

Weak-line T Tauri stars are pre-main sequence stars that have hydrogen lines in emission, but with an  $\text{H}\alpha$  equivalent width under  $10 \text{ \AA}$  (the equivalent width is the width the line would have on supposing the line emission peaks at the same level as the stellar continuum). In 1978, George Herbig described them as *post T Tauri stars*, having finished their formation and now heading towards the main sequence.

Consequently, large numbers were discovered in X-ray surveys with the Einstein Observatory and ROSAT satellites. These stars were previously not identified as young stars because they also lacked excess infrared and UV emission. Follow-up observations of their radial velocities showed that these serendipitous sources did indeed belong to nearby star formation regions. Locating them on the Hertzsprung-Russell diagram, it became apparent that many of them were not older than the CTTSs. Assigning ages to them according to evolutionary models (Fig. 9.2), it was also clear that these non-disk objects dominate the population of young stars older than 1 Myr.

Due to their unveiling, in the physical sense, the WTTs were called *naked* T Tauri stars. In general, we refer to the class as weak-line T Tauri star but note that not all WTTs are stark naked: there are WTTs which are not NTTs. Classification is never completely satisfying. Firstly, higher mass G stars have high continuum fluxes which can veil intrinsic hydrogen line emission. Secondly, stars with optically thick disks do not necessarily show strong  $\text{H}\alpha$  emission, classifying them as WTTs, yet not considered

to be NTTs.

Among stars which are optically visible, we can extract candidate young stars by searching for the presence of lithium in their atmospheres. Lithium is depleted in stars as they age. It is a fragile element and is destroyed at the temperatures reached at the base of the convection zone. A temperature of  $\sim 2.5 \times 10^6$  K is necessary. Convection mixes the material and transports it between the surface and interior. This process, called convective mixing (§9.6), is efficient at reducing the surface lithium abundance. We thus employ lithium absorption lines (specifically a strong Li I 6707 Å absorption line) to help identify and confirm young stars.

### 9.1.3 *Outbursts: FU Ori objects*

Certain stars in star formation regions have been found to increase in brightness by several orders of magnitude over a period of months to years. These are called FU Orionis eruptive variables, or FU Ori objects. The luminosities can reach a few hundred  $L_{\odot}$ . The two best studied members of the class, FU Ori and V1057 Cyg, have both exhibited increases in optical brightness by 5–6 mag on timescales of about a year, followed by gradual fading. The frequency of FU Ori eruptions is still poorly known. The eruptions may occur many times during the T Tauri phase of a star, suggesting mean times of  $10^4$ – $10^5$  yr between successive outbursts, with decay times of perhaps several hundred years.

Some objects are now accepted as members of the FU Orionis class only because they are spectroscopically very similar to the classical FU Orionis stars even though no eruption has been observed. The classification scheme is now based on other properties of the objects. We use the presence of the overtone bands of CO, observed as deep broad absorption in the infrared, to identify FU Ori disks. The band emission is produced in the hot inner disk through many overlapping lines from the vibrationally excited molecule. In addition, post-eruption optical spectra show peculiar supergiant F and G type stellar spectra, with blue-shifted shell components, and ‘P Cygni line profiles’ in  $H\alpha$ , taken as evidence for outflow. Although these objects are in an early stage of evolution, it is appropriate to introduce them here since their properties are closely linked to their disks. These objects, such as L1551 IRS5, also produce jets and bipolar molecular outflows. The high luminosities suggest accretion rates exceeding  $\sim 2 \times 10^{-6} M_{\odot} \text{ yr}^{-1}$ .

A model in which accretion through the circumstellar disk is greatly increased can explain many observed peculiarities of FU Orionis objects,

including the broad spectral energy distributions, the variation with wavelength of the spectral type and rotational velocity, and many ‘double-peaked’ spectral lines in the optical and the near-infrared. Increased mass transfer through the disk may be triggered by a thermal instability or by the close passage of a companion star. Origins for this class of object will be further discussed below (§9.5).

## 9.2 Class II and Class III Objects

Class II and Class III protostars are characterised by energy distributions which peak in the near-infrared and optical regions of the spectrum. The emission is dominated by that directly from stellar photospheres.

Class II sources are less embedded than Class I sources. Their spectral energy distributions (SEDs) are broader than that corresponding to single blackbodies. The excess emission extends across mid-infrared wavelengths with a power-law infrared spectral index of  $-1.5 < \alpha_\lambda < 0$ . This emission arises from circumstellar material with temperatures in the range 100 K to 1500 K and is normally associated with a disk system, without a significant envelope. Their bolometric temperatures lie in the range  $650 \text{ K} < T_{bol} < 2,800 \text{ K}$ . When observed in the optical, Class II sources typically possess the signatures of CTTSs, and CTTSs generally possess Class II type SEDs.

Class III SEDs correspond to reddened blackbodies. In this case, the emission is associated entirely with a photosphere, with no contribution from an optically thick disk. Without an infrared excess, the radiated energy decreases more steeply longward of  $2\mu\text{m}$  than Class II SEDs, with  $\alpha_\lambda < -1.5$ . Foreground dust may still provide considerable extinction, which acts to redden the object through the preferential obscuration of the high-frequency end of the intrinsic blackbody. Class III sources produce very little H $\alpha$  emission, so officially defining them also as weak-line T Tauri stars.

## 9.3 Location and Number

Young stars may be found distant from their apparent natal cloud or not even associated with any recognisable cloud. Some may well form individually or in isolated systems, as part of a distributed mode of star formation. Others may form in molecular clumps, in a clustered mode.

The age of individual T Tauri stars is sensitive to the chosen model. They can be tentatively placed on the classical Hertzsprung-Russell diagram and located along evolutionary tracks derived from pre-main-sequence models (Fig. 9.2). CTTs are so found to have typical ages of  $1\text{--}4 \times 10^6$  yr while WTTs take a wider range of ages  $1\text{--}20 \times 10^6$  yr. Most Class III sources are, however, older than  $5 \times 10^6$  yr, and may well be classified as *post* T Tauri stars.

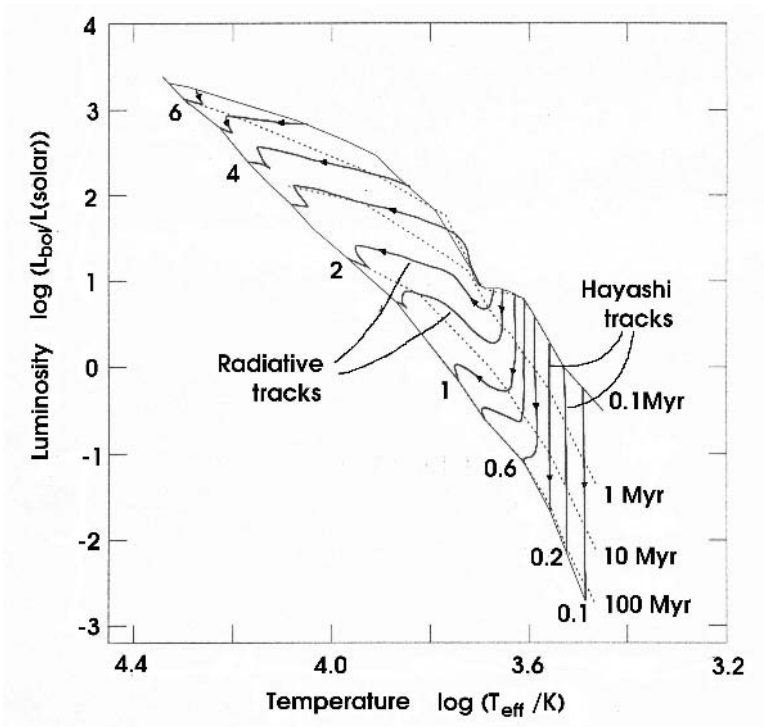


Fig. 9.2 The Hertzsprung-Russell diagram for T Tauri and intermediate mass stars (adapted from work by Palla & Stahler, 1998).

The number of Class III sources is difficult to ascertain since their properties are not so outstanding. As strong X-ray sources, their X-ray emission provides the best means for a census (§9.7). They appear to be at least as populous as Class II sources and to extend further beyond the outskirts of the star formation regions, consistent with their age.

## 9.4 Accretion

### 9.4.1 *General characteristics*

There are three stages in the transition from an envelope-dominated to a star-dominated system. Firstly, quite early in the evolution of a forming star, the disk-protostar system is still surrounded by an infalling envelope. The envelope generates the far-infrared SED. At longer wavelengths, the infalling envelope becomes optically thin, and the SED is dominated by disk emission. At this stage, radiation from the infalling envelope is one of the most important heating mechanisms of the disk and has to be included to understand the long wavelength SEDs of embedded stars.

In the second transition phase, the disk and young star are surrounded by a tenuous dusty envelope that scatters stellar radiation onto the disk. This radiation can significantly heat the outer regions of the disk. Finally, in a more evolved phase, it is expected that the material surrounding the disk-star system becomes negligible.

Why a disk? The puzzle was to fit a large amount of circumstellar material around a CTTS without obscuring it. If distributed spherically, the young star would not be visible in the optical. It was therefore suggested that it is distributed in a geometrically thin disk. A disk was, in any case, expected to form as accreting material falls within the centrifugal barrier. The envelope material will land onto the disk and must subsequently accrete from there onto the central object. Direct proof eventually came through the Hubble Space Telescope which imaged spectacular disk-like silhouettes on a background nebula illuminated by stars in the Orion cloud.

Many questions are only half answered. Can a disk explain the infrared excess? What happens to the angular momentum of the disk to allow the material to accrete onto the star? Does the material crash or settle onto the star?

### 9.4.2 *Accretion disk specifics*

We first focus on what type of disk can reproduce the observed infrared excess. Specifically, we have to match the power-law wavelength dependence of the SED. Physically, we hope to learn about the disk physics although we actually only directly model the temperature structure.

The basic model is that of a disk which is geometrically thin but optically thick. The model disk is dissected into a series of annuli, the surface

area of an annulus of radial width  $\Delta R$  being  $2\pi R\Delta R$ . The spectrum from each annulus corresponds to a blackbody with a specific temperature. We take a radial temperature distribution  $T(R)$ . The emergent spectrum is then the superimposed contributions of the annuli. The temperature distribution depends on the heat released from within the disk. If we take a distribution of the form  $T(R) \propto R^{-n}$ , so that positive index  $n$  implies that the inner disk is hotter than the outer disk, then the blackbody luminosity from a disk annulus is

$$L(R) \Delta R = 2\pi R\Delta R \sigma T^4. \quad (9.1)$$

The temperature difference across an annulus is  $\Delta T/\Delta R \propto R^{-n-1}$ . Substituting for  $R$ :

$$L(T) \propto T^{3-\frac{2}{n}} \Delta T. \quad (9.2)$$

Employing Wien's law, Eq. 6.2,  $T \propto \nu$ , the predicted SED slope possesses a power law slope as defined by Eq. 8.1 of

$$\alpha_{\lambda,disk} = \frac{2}{n} - 4. \quad (9.3)$$

Therefore, the predicted SED is indeed a power law directly related to the temperature distribution across the disk. For Class II sources, the most common values observed lie in the range  $\alpha_{\lambda} \sim [-0.4, -1.0]$ , which implies a range of  $n \sim [0.56, 0.67]$ . The question now is what model for the disk produces such a temperature structure?

First, we consider the standard theory of an 'active' accretion disk. The properties of a standard disk, which channels material from an envelope or mass-losing companion onto the star, are well known. We ignore the pressure in the disk, whether thermal or turbulent, and so balance the centrifugal force with gravity at radius  $R$ , given an angular rotation  $\Omega$  and a dominant central mass  $M_*$ :

$$R\Omega^2 = \frac{GM_*}{R^2}. \quad (9.4)$$

This implies that the disk does not rotate like a solid body. It is a sheared flow with rotation rate  $\Omega = (GM_*/R^3)^{1/2}$ .

We can now understand why the material in the disk will fall inwards despite the necessary conservation of total angular momentum. Viscous forces are created in the disk due to the shear, as described in §5.3. Viscosity leads to dissipation of flow energy into thermal energy i.e. the disk is heated. It also leads to outward transport of angular momentum and

a redistribution of energy: the specific angular momentum,  $\Omega R^2 \propto R^{1/2}$ , decreases with radius instead of being conserved.

In a steady-state, the rate at which mass flows inwards is just the rate at which we supply the disk with new material. The dissipation through viscosity should adjust to meet the demands: it can redistribute angular momentum and energy but not alter the totals. This property of the viscous force was also found in the discussion of shock fronts (see §5.5). If the mass supply is high, then the disk will be massive so that molecular friction can cope. If the mass supply is too high, however, then molecular viscosity is ineffective and some form of anomalous viscosity must take over. Turbulent viscosity is generated by MHD instabilities (see §9.5).

Geometrically, the disk may be thin but it has a thickness which is not constant. We define the thickness by the pressure scale height  $H(R)$ , a function of the disk radius  $R$ . If the spinning disk is assumed to be in vertical hydrostatic equilibrium, then a vertical pressure gradient pushing up is balanced by the small component of radial gravity which pushes down. This equilibrium implies

$$H/R = c_s/v_d \quad (9.5)$$

where  $v_d$  is the Keplerian rotation speed  $\Omega R$ .

Finally, if the disk mass is so high that self-gravity becomes important, then gravitational instability prevails and tidal torques transport the angular momentum outwards and the mass inwards. Gravitational instability also leads to fragmentation and the formation of bound objects: brown dwarfs or planets. For a disk whose potential is dominated by the protostar and whose rotation curve is therefore approximately Keplerian, instability sets in when the disk surface density  $\Sigma$  is sufficiently large. Analysis yields the condition for instability:

$$\Sigma > \frac{c_s \Omega}{\pi G Q_c}, \quad (9.6)$$

where  $Q_c$  is called the critical value of the so-called Toomre parameter (of order unity). Putting the disk mass  $M_d \sim \pi R_d^2 \Sigma$  and using Eq. 9.5, we obtain the instability condition

$$M_d > \frac{H}{R} M_*. \quad (9.7)$$

Therefore, a thin disk which contains a significant mass fraction will be unstable. For the outer parts of YSO disks  $H/R \sim 0.1$ , and thus a massive

disk is required for instability.

Remarkably, we already know enough to predict the temperature distribution. The energy for the local dissipation ultimately derives from the gravitational potential. The heating extracted directly from the infall is at the rate

$$\dot{E} = \dot{M} \frac{\Delta R}{R} \frac{GM}{R}. \quad (9.8)$$

This is mollified by the change in rotational energy and modified by the viscous transport of energy. We also place an inner boundary condition where the dissipation rate falls to zero. It turns out that the energy release maintains the above form at large radii and can be written in more detail as

$$\dot{E} = \frac{3GM\dot{M}}{2R^2} \left[ 1 - \left( \frac{R_*}{R} \right)^{1/2} \right] \Delta R. \quad (9.9)$$

Integration over the entire disk yields a total dissipation of  $GM\dot{M}/(2R_*)$ , exactly one half of the available potential gravitational power. The other half remains in the form of the inner spinning disk, from where it must be somehow extracted. Hence, the disk is only half the potential story.

The effective temperature of the optically thick disk is then given by the formula for a blackbody, Eq. 6.4, taking into account that the disk has two surfaces,  $\dot{E} = 4\pi R\Delta R \sigma_{bb} T_{disk}^4$ :

$$T_{disk}^4 = \frac{3GM\dot{M}}{8\pi\sigma_{bb}} \frac{1}{R^3} \left[ 1 - \left( \frac{R_*}{R} \right)^{1/2} \right]. \quad (9.10)$$

In other words,  $T_{disk} \propto R^{-3/4}$  over the extended disk.

This is not quite what we were hoping for: a standard disk is predicted to have a radial temperature distribution with  $n = 0.75$  whereas the Class II SEDS generally imply a shallower fall-off in temperature,  $n \sim [0.56, 0.67]$ .

A second problem is also raised by the other half of the story: while half the disk accretion power may appear as the infrared excess, the other half must be lost in a small boundary layer between the disk and the star. This high power from a small area would produce ultraviolet excess emission which should be as strong as the infrared excess. Indeed, an ultraviolet excess is observed. However, the excess is far less than the infrared excess for many well-studied systems. This suggests that the mass accretion rate onto the boundary layer is actually lower than that through the disk, which would cause material to pile up in the inner disk. Such a situation cannot

last long. This leads us to suspect that we have not taken everything into account.

The solution appears to lie in the fact that we assumed the disk to be isolated. It is, in fact, exposed to the central star. A major heating agent in many CTTSs will be irradiation: a passive disk is heated on processing of the incident radiation. For a flat disk, however, this turns out to yield the same temperature distribution as predicted from the standard model. The reason for this is that the stellar luminosity  $L_* = 4\pi R_*^2 \sigma_{bb} T_*^4$  is diluted by  $(R_*/R)^2$  due to the usual spherical expansion plus a further  $R_*/R$  due to the grazing incidence of the radiation. In detail, the effective disk temperature due to the irradiation is given by

$$T_i^4 = \frac{2T_*^4 R_*^3}{3\pi} \frac{1}{R^3}. \quad (9.11)$$

Therefore, on comparing Eqs. 9.10 and 9.11, the irradiation dominates what we measure from the entire disk provided the accretion rate is less than

$$\dot{M}_{crit} = 2 \times 10^{-8} \left( \frac{T_*}{4000 \text{ K}} \right)^4 \left( \frac{R_*}{2R_\odot} \right)^3 \left( \frac{M_*}{0.5M_\odot} \right)^{-1} M_\odot \text{ yr}^{-1}. \quad (9.12)$$

For a flat disk, however, at most 25% of the stellar radiation is directed sufficiently downwards to intercept the disk (none from the pole and 50% from the equator). Yet, for many CTTSs the infrared excess accounts for as much as 50% of the total stellar radiation (e.g. for T Tau itself).

What accretion rate is predicted for the disk? An anomalous viscosity which generates the turbulent transport of angular momentum, might scale in proportion to the disk scale height and sound speed according to §5.3. We thus take the viscosity to be  $\alpha_{ss} c_s H$ , a prescription for a standard disk, first invoked by Shakura & Sunyaev in 1972. Then, using the above analysis, the accretion rate can be written

$$\dot{M}_{disk} = 3\alpha_{ss} \frac{c_s^3}{G} \left( \frac{M_d}{0.01M_*} \right) \left( \frac{0.1R_d}{H} \right). \quad (9.13)$$

Written in this form, one can see the type of disk necessary to convey the envelope mass onto the protostar, given the supply from the envelope given by Eq. 8.5.

If the disk is flared, so that the disk ‘photosphere’ curves away from the disk midplane, the cool outer regions receive more stellar radiation and so are gently warmed, exactly as required to produce a shallower temperature gradient. Moreover, the extra heating contributes to increasing the height

of the disk and so to increasing the exposure. As we have discussed above, a flared disk is actually predicted. Given the vertical scale height  $H \sim c_s/\Omega$  from Eq. 9.5 and substituting for  $c_s \propto T_{disk}^{1/2}$  and  $\Omega$ , yields  $H/R \propto R^{1/8}$  – a very gradually flaring disk exposed to the protostar.

### 9.4.3 The star-disk connection

It was long thought that the disk continued all the way down into the star and disk material joined the star via a hot boundary layer where half the accretion energy would be released. There is now a large and growing body of evidence which suggests this does not happen. Instead, the current paradigm asserts that the stellar magnetic field is strong enough to disrupt the inner disk. The disk is truncated and the material is then diverted along the magnetic field, forced to accrete nearly radially onto the star, as shown in Fig 10.4.

A key prediction of the magnetospheric infall scenario is the formation of a shock wave on the stellar surface. Material reaches the surface at supersonic velocities, approaching the surface at a free-fall velocity of several hundred kilometres per second. Therefore, close to the surface the gas produces a strong standing shock wave, in which the kinetic energy of the infalling stream is transformed into random thermal motions. It is thought that radiation from the shock, half reprocessed by the stellar surface, is responsible for the UV and optical continuum excess which veil the absorption lines in CTTSs.

Magnetospheric accretion also implies that there is an inner hole in the disk. The disk is truncated close to or inside the co-rotation radius, which is typically at radii 3–5  $R_*$ . There will then be no contribution to the infrared spectrum corresponding to emission from gas at temperatures exceeding about 1000 K. Such ‘inner holes’ would thus correspond to a sharp drop in emission in the near infrared. This effect is observed although other contributions and geometric effects can hide it.

The peculiar spectral characteristics of classical T Tauri stars are now usually interpreted in terms of magnetospheric accretion. The densities in the accretion column,  $10^{10}$ – $10^{14}$   $\text{cm}^{-3}$ , are typical of the solar chromosphere and transition region. The infalling material is detectable as a redshifted absorption feature in the wings of prominent broad emission lines. The magnetic field, and hence the accretion streams, will rotate with the star, leading to variability of the strength and velocity of the absorption component. Observations of this shifting absorption can be used to constrain the

geometry of the inner regions of the system, and hence the geometry of the magnetic field.

The accreting column can be divided into three regions: the shock and post-shock regions, the photosphere below the shock, and the pre-shock region above it. The shocked gas is heated to a high temperature, of order  $10^6$  K, which then decreases monotonically as the gas settles onto the star. It emits mostly soft X-rays and UV. Half of this radiation is sent to the photosphere below and half to the pre-shock region above. In turn, a fraction of the radiation from the pre-shock gas is emitted back toward the star, adding to the radiation from the post-shock gas to heat the photosphere. The flux of radiation incident on the photosphere heats the gas to temperatures higher than the relatively quiescent surrounding stellar photosphere, producing a hot starspot.

The origin of the veiling in the accretion shock column, rather than in a boundary layer, has crucial energetic consequences. In the immediate vicinity of the boundary layer, disk material is rotating at nearly Keplerian velocity at the stellar radius; to enter the star, the material has to slow down and emit this kinetic energy, which amounts to nearly half of the accretion luminosity while the disk emission accounts for the other half. In contrast, in magnetospheric accretion, material falls from several stellar radii, so that the energy released is almost the entire accretion luminosity. Therefore, the intrinsic disk emission is only a small fraction of the accretion luminosity.

## 9.5 Class and Disk Evolution

As it is unfolding in this chapter, a young star undergoes a complex development. It involves the evolution of several components within a single system, and the transfer of mass and radiation between the components.

The mass accretion rates for CTTSs derived from veiling measurements lie in the wide range of  $4 \times 10^{-9}$  to  $10^{-7} M_{\odot} \text{ yr}^{-1}$ , much lower than the rates derived for Class 0 and Class I protostars. Modelling the accretion column and calibrating emission lines in the near-infrared, has allowed us to also tentatively assign accretion rates onto even optically-obscured protostars. This method indicates that many Class I protostars appear to be slowly accreting from their disks even though the envelope is supplying material at a high rate onto the outer disk (see §8.10). In Taurus, Class I disk accretion rates occupy a wide range around  $\sim 10^{-7} M_{\odot} \text{ yr}^{-1}$  whereas, on average, the infall from the envelopes proceeds at the rate

$\sim 3 \times 10^{-6} M_{\odot} \text{ yr}^{-1}$ . This anomaly is termed the luminosity problem for Class I sources.

One suggested resolution is that mass indeed accumulates in the outer disk. When sufficient mass has accumulated, the disk becomes gravitationally unstable, with subsequent strong and abrupt accretion until the excess disk mass has emptied. This would account for the outbursts which identify FU Ori objects (see §9.1.3). A more likely cause for the outbursts is that of thermal instability in the inner disk which is expected when the mean accretion rate is quite high – above  $10^{-6} M_{\odot} \text{ yr}^{-1}$ . An objection to such scenarios is that very few FU Ori disks have been found so far although protagonists will claim that they are still deeply obscured. If common, then it is no longer possible to locate young stars unequivocally on evolutionary tracks.

The infall phases correspond to the Class 0 and Class I protostars. The mean mass left to accrete during the Class II phase is just  $\sim 0.01 M_{\odot}$ . Nevertheless, the early accretion is probably episodic with short periods of high accretion.

Despite the outbursts, the long-term accretion rate appears to decrease with age from Class I to Class II sources. Using statistics, we derive a relationship of the form

$$\frac{\dot{M}}{10^{-6} M_{\odot} \text{ yr}^{-1}} \sim \left( \frac{t_{age}}{10^5 \text{ yr}} \right)^{-1.5}, \quad (9.14)$$

according to the present data, which is probably strewn with errors. Nevertheless, if we assume that exactly this mass is fully supplied by the disk, we can compare the predicted disk mass with that derived directly from submillimetre observations of the dusty disks. The two are in reasonable agreement (for an appropriate dust opacity in the disk, needed to convert dust mass into gas mass).

Can we explain the above power-law evolution of mass accretion? For the disk to evolve, angular momentum must be transported. Little can be transferred to the star itself without it reaching break-up speeds. We have essentially three choices, as follows:

- The disk gas coagulates into dense bodies which then sweep clear the remaining gas.
- A disk wind is driven by centrifugal forces, removing a high fraction of angular momentum.
- Disk viscosity transfers angular momentum outwards.

On the largest scales, the third choice is favoured. In this case, as the system evolves, the disk grows in size in order to incorporate more angular momentum into less material. We note from Eq. 3.17 that the angular momentum is  $J_d \propto M_d \Omega_d R_d^2$  in a disk of evolving mass  $M_d$  and radius  $R_d$ . From Eq. 9.4, we can substitute  $\Omega_d \propto R^{-3/2}$  to yield  $J_d \propto M_d R_d^{1/2}$ . Thus, most of the angular momentum lies on the outskirts of the disk, and, as the disk loses mass, it expands at the rate  $R_d \propto M_d^{-2}$ , conserving angular momentum.

The evolutionary timescale  $t_{visc}$  depends on the viscous transport. As discussed in §5.3, this is a slow diffusion process with

$$t_{visc} = R^2/\nu. \quad (9.15)$$

for a rotating disk. To proceed from here we now need a viscosity prescription. Given the shear, we expect that turbulent viscosity will dominate. This takes the form of Eq. 5.5:  $\nu_e = \lambda \times v$ . We substitute turbulent length and velocity scales appropriate for the disk: the scale height and sound speed and take an efficiency factor  $\alpha_{ss}$ , to yield

$$\nu_e = \alpha_{ss} c_s H \propto c_s^2(R)/\Omega(R) \propto TR^{3/2} \quad (9.16)$$

to describe a standard or ‘alpha’ disk model. Substituting  $T \propto R^{-0.6}$  (see above), then  $\nu_e \propto R^{0.9}$ . The timescale thus predicted from disks we see, interpreted as standard disks, is  $t_{visc} \propto R^{1.1}$ . This implies that as a disk expands, the evolutionary time increases and, from angular momentum conservation, the disk mass  $M_d \propto t^{-1/2.2}$ . This then yields a mass transfer rate of  $\dot{M}_d \propto M_d/t \propto t^{-1.46}$ . This is remarkably close to the relationship we derived between accretion rates and estimated ages of Class 1 and CTTSs (Eq. 9.14), suggesting that we might be reaching a fully consistent basis for understanding disk behaviour.

The physics behind the viscosity has attracted much attention. We have not been specific about the cause of the disk turbulence. We require a hydrodynamic or magnetohydrodynamic instability to disturb the sheared disk and tap its energy. Values for the disk parameter  $\alpha_{ss} \sim 0.01$ – $0.1$  are consistent with observations. One instability mechanism is the magnetorotational instability (MRI), also called the Balbus-Hawley instability after the discoverers. This is based on the interchange of the positions of magnetic field lines which thread vertically through the disk, leading to a loss of equilibrium. If the disk mass is sufficiently large (see Eq. 9.7), then self-gravity is relevant. Self-gravity will generate density structure in the form

of spiral arms. Gravitational torques may then simulate a viscosity. The viscous heating may increase the sound speed and so hold the disk mass to the critical value  $M_d \sim Mc_s/R_d$ .

## 9.6 Interiors

Theory predicts that a low mass star does not progress from a dim and cold beginning to become a luminous and warm star in a steady increasing fashion. On the Hertzsprung-Russell (H-R) diagram, the evolutionary path is seen to perform a detour along what is termed a Hayashi track (Fig. 9.2). Here we explore the reason for the detour.

When the envelope has been shed, the young star can be observed in the visible. Since it is highly opaque, the gravitational energy released through contraction cannot easily escape. It possesses a photosphere, interior to which photons are trapped. For this reason, it is a quasi-static object in which the internal pressure is very close to supporting the object against gravity. This state is called hydrostatic equilibrium.

As the object slowly contracts, gravitational energy is released. Half of this energy remains as internal energy, helping to maintain the pressure support (a requirement of the virial theorem (see Eq. 4.4)). The other half escapes from the photosphere as radiation.

A major difference between young stars is brought about by the manner in which energy is transferred to the surface. It was originally thought that the internal structure is simply determined by the means by which the photons would leak out. This is the process of radiative diffusion: the journey of a photon is a random-walk, being repeatedly emitted and absorbed by the atoms.

T Tauri stars behave differently. It was shown by Hayashi in 1966 that their interiors begin by being in a state of convection. This means that if a packet of gas is displaced radially its displacement will not be suppressed but will grow. For example, a packet of gas rising from deep in the star into a lower pressure region nearer the surface will expand. If it expands sufficiently, it will remain buoyant in its new surroundings and continue to rise. Convection thus redistributes the energy by circulating the gas.

Convection becomes a very effective energy transport mechanism in young stars as soon as there is a steep temperature gradient to drive it. This occurs in T Tauri stars because radiative diffusion cannot cope with the prodigious internal energy release as the young star becomes opaque.

The internal temperature rises, setting up convection currents. During this phase, the energy release no longer depends on the efficiency of internal transport but just on how quickly the surface layer can liberate it. The surface opacity is, however, very sensitive to the temperature, providing a positive feedback which tends to stop the temperature from changing. The result is that, as the star contracts, the surface temperature stays approximately constant while the luminosity falls as  $L \propto R_*^2$  (i.e. according to the blackbody formula, Eq. 6.4). This yields the near vertical evolution on the H-R diagram shown in Fig. 9.2.

As the luminosity falls, the opacity and temperature gradients fall in the inner regions. Consequently, the core of the star becomes radiative. The size of the radiative core grows, leaving a shrinking outer convective zone. In this radiative phase, the internal radiative diffusion, rather than the surface opacity, controls the energy loss. The contraction is now slow but, because the star gradually contracts, the internal energy must rise (according to the virial theorem) and so the central temperature rises also. The result is that the luminosity increases. Both the increase in luminosity and the contraction ensure that the temperature rises relatively fast. The end result is a quite horizontal evolution on the H-R diagram, along a ‘radiative track’.

There will probably always be considerable uncertainty surrounding pre-main sequence evolution. Besides well-known uncertainties in the opacity and in the means used to model convection (mixing-length theory), the accretion of residual disk gas is important. Nevertheless, the theoretical tracks provide masses and ages for individual objects which are roughly consistent with other estimates. We estimate that a solar-type star will spend 9 Myr descending the Hayashi track and then 40 Myr crossing to the main sequence on a radiative track. In contrast, stars with mass above about  $2.5 M_\odot$  possess no convective track while those with a mass exceeding perhaps  $6 M_\odot$  cannot be considered to experience such pre-main sequence phases. Instead, they probably finish their main sequence life before a contemporary low-mass star has contemplated it.

## 9.7 Giant Flares, Starspots and Rotation

The surfaces of T Tauri stars are extremely active. The activity provides further clues as to how the young stars evolve. However, many results do not as yet fit neatly into any prevailing scenario.

T Tauri stars are strong X-ray sources. The X-ray emission is roughly correlated with the bolometric luminosity by  $L_X \sim 10^{-5} - 10^{-3} L_{bol}$ . In comparison,  $L_X/L_{bol} \sim 10^{-6}$  for the Sun and  $L_X/L_{bol} \sim 10^{-7}$  for massive stars. The radiation is continuous in wavelength, generated from the thermal Bremsstrahlung mechanism introduced in §2.3.1, except in this case from a very hot plasma (ionised gas) with a characteristic temperature of 1 keV, or  $10^7$  K.

The origin of the X-rays lies in strong magnetic activity. The interior convection and rotation lead to differential rotation within the star. This generates magnetic flux through a dynamo mechanism. The flux is released sporadically with magnetic field-line reconnection significant, disrupting and heating the atmosphere. Considerable evidence points to this solar-like paradigm. In particular, variations in the X-ray luminosity by factors of a few over months and factors of 10 over days have been recorded. The variations are flares: an abrupt rise followed by an exponential decline. The temperature falls as the flux falls, consistent with a cooling plasma. The flares are gigantic, sometimes stretching out over several stellar radii.

In general, WTTSs are stronger than CTTSs in the X-rays. This is at least partly because the CTTSs are fairly heavily absorbed, hence not found so easily detected in X-ray surveys. However, there are probably intrinsic differences. In addition, protostars and brown dwarfs also appear to be X-ray sources, especially Class I protostars. Moreover, peak X-ray luminosities can be extremely high. The full meaning of all these results is yet to be assessed.

Painstaking monitoring campaigns have revealed that most T Tauri stars display periodic luminosity variations from a fraction of a day up to about 10 days. The variations are often approximately sinusoidal, consistent with large spots on the surface of rotating stars. The area occupied by the spots can be between 2–30% of the surface area. In WTTSs, spectroscopic fluxes indicate that the spots are cooler regions and an explanation in terms of convection and magnetic activity is appropriate. The spot interpretation is confirmed through high resolution spectroscopy of individual absorption lines in the photospheres. The width of these lines corresponds to the Doppler shifts caused by the rotation. Clearly, for those stars observed along the rotation axis, we will detect neither the spot-generated variations nor the rotation speed. For the majority, however, we have measurements of the rotation period,  $P$ , and the radial component of the rotation speed,  $v \sin i$  ( $i$  is traditionally used to denote the orientation of the rotation axis to the observer). The radii of the stars are also given from

the blackbody component of the luminosity and temperature. We thus obtain comparable sets of data for the speed of rotation which confirms the periodic variations to be caused by surface blemishes. .

The spots on classical T Tauri stars are hotter than the surface. This implies an alternative origin linked with high-speed infall from the accretion disk, as discussed in §9.4.3. The spots are thus directly connected to the spinning disk.

This brings us to a long-standing ‘conundrum’: where does the angular momentum go during the evolution of a young star? Having contracted from their natal cores, young stars should spin close to their break-up speeds (i.e. the rotation speed should approach the gravitational escape speed). In fact, their typical rotation speeds of 10–25 km s<sup>-1</sup> are only about 10% of their break-up values. Subsequently, the young stars should spin up considerably as they accrete from the rotating disk and contract along Hayashi tracks. In fact, they are still slow rotators when they eventually arrive at the main sequence.

There is some evidence for a spin up. In the Taurus region, the distribution of rotation periods is bi-modal with the CTTS possessing periods 5–8 days and the WTTSs periods 1–4 days. The gap between these ranges is the subject of much speculation. For T Tauri stars in the Orion Nebula Cluster the bi-modal distribution is again present but only for stars with masses exceeding  $\sim 0.25 M_{\odot}$ . Furthermore, there is a subset of young stars rotating with a high fraction of the break-up speed.

How can we answer the conundrum? In very young systems, it is thought that the angular momentum of the star is strongly regulated by the circumstellar disk. The stellar magnetic field threads the disk, truncating it inside the co-rotation radius (i.e. where the disk rotation period is less than the stellar rotation period, perhaps at about  $5 R_{*}$ ). The accretion then continues along the field lines, producing hot surface zones at high latitudes. Simultaneously, magnetic torques transfer angular momentum from the star into the disk. Such a disk-locking or disk-braking mechanism seems essential to explain the low angular momenta of CTTSs. Later, when the evolution has slowed, magnetic wind braking can be more effective.

## 9.8 Summary

There are several defining moments in the life of a young star of mass under  $\sim 2.5 M_{\odot}$ . One special transition occurs when it loses its opaque accretion

disk. The lifeline to the maternal cloud is irrevocably broken and it stands alone, subject to its changing interior structure. Surface blemishes and giant flares testify to internal upheavals in an exaggerated version of the adult star that it develops towards.

It had already experienced a more dramatic transition for us when it lost its envelope, becoming exposed to visible light. The accretion disk and photosphere then became open to a deep inspection of their atomic compositions. For the star itself, the transition was less critical since the circumstellar disk remained in place, providing an outlet to release its rotational energy. Throughout, however, the disk needs to be churned to feed the star: some form of turbulence separates the spin from the gas.

There is a remarkable twist to the story. Another activity has been ongoing and evolving while all the transitions since the birth have been taking place. This activity – the bipolar outflow – has radically altered many of our interpretations: we have underestimated the ability of a protostar to influence its own environment.

